www.sciencemag.org/cgi/content/full/1167625/DC1

Supporting Online Material for

Greatly Expanded Tropical Warm Pool and Weakened Hadley Circulation in the Early Pliocene

Chris M. Brierley, Alexey V. Fedorov,* Zhonghui Liu, Timothy D. Herbert, Kira T. Lawrence, Jonathan P. LaRiviere

*To whom correspondence should be addressed. E-mail: alexey.fedorov@yale.edu

Published 26 February 2009 on *Science* Express
DOI: 10.1126/science.1167625

This PDF file includes:

SOM Text

Figs. S1 to S3

Tables S1 to S3

References

Paleo Observations in Fig. 1: We generated about 900 alkenone SST measurements in this study, covering the time interval between ~1.8 Ma and ~4 Ma from ODP Site 1012 (32º17'N, 118º24'W). We sampled sediments every 15 cm for the interval 126-187 m and every 20 cm for the remaining core (187-282 m), for an average 3-kyr resolution. Pliocene SST changes at ODP 1012 were estimated based on the alkenone unsaturation index ($U^{K'}_{37}$), defined as $U^{K'}_{37}=C_{37:2}/(C_{37:2}+C_{37:3})$, where $C_{37:2}$ and $C_{37:3}$ are the concentrations of di- and tri-unsaturated C_{37} alkenones (*S1*). Reproducibility for $U^{K'}_{37}$ is better than ±0.005, corresponding to a temperature uncertainty of ± 0.15ºC using the calibration of Prahl et al. (*S1*). The Pliocene chronology at ODP 1012 is based on 5 biostratigraphic control points from the ODP initial report (*S2*), and further refined by correlating similar features in both this record and the SST record from ODP 846 (*10*). The newly generated Pliocene SST record from ODP 1012 was then combined with existing records from ODP 1012 (*S3*) and ODP 846 (*10*) to reconstruct the meridional SST gradient in the eastern Pacific.

Paleo Observations in Fig. 2: Fig. 2 combines currently available proxy SST data from Mg/Ca and alkenone techniques for the early Pliocene. Specifically for this paper we produced alkenone proxy temperatures for ODP sites 982, 1090, and DSDP 607 (in addition to ODP 1012) using the same methodology as described above. We also utilized results of previous studies *(6-10, 17-21).* The chosen period of the reconstruction, around 4-4.2 Ma, coincides with the time when the east-west temperature gradient along the equator almost fully collapsed (*6,* fig. 1d) and is in the middle of the early Pliocene warm interval.

Our reconstruction of the meridional SST distribution in the open ocean in the Pacific (roughly along the dateline) invokes several temperature adjustments, because of scarcity of available temperature data. One important basis of these adjustments is that the data indicate very weak temperature variations, both zonal and meridional, within the tropical warm pool. For example, the maximum SST for this time interval is roughly 28.5^{o}C (in the equatorial region), while the temperature in the upwelling zone off the coast of California at 33^{o}N is 26^{o}C, so we can assume that the temperature in the middle of the Pacific at this particular latitude will lie between these two numbers, say 27^{o}C. Other important assumptions include the assumptions that modern differences between Atlantic and Pacific temperatures at given latitude persisted throughout the Pliocene and that the climate cooled between the early to mid-Pliocene by roughly 2^{o}C (which is consistent with available data). The detailed description of the adjustments is below:

(a) If a data point originates from a coastal or equatorial upwelling region, we add a correction of +1^{o}C, in order to estimate the temperature away from the coast. This correction is rather conservative. If tropical temperatures in the early Pliocene did not exceed 28-29ºC, as suggested by available data, the upper bound on this correction is 2-3ºC, which would raise our SST estimates at around 30ºN even higher.
(b) If a data point is from the northern Atlantic (to the north of 35ºN), we subtract 4ºC to allow for the difference between the Atlantic and Pacific. At present, surface waters in the North Pacific are generally 2 to 7ºC colder than in the Atlantic at the same latitude. The chosen correction (4ºC) gives a very good agreement at 50ºN where we have data both from the Pacific and the Atlantic.
(c) For the data point from the southern Atlantic (at 42ºS) we add 4ºC, which corresponds to the modern difference between this location in the Atlantic and the Pacific dateline temperature.

(d) For the data point from the northern Pacific (at 50ºN) we add 1ºC, which corresponds to the modern difference between this location and the dateline temperature.
(e) Finally, if a data set extends only to 3 Ma, we add 2ºC to allow for climate cooling between 4 to 3Ma, since most of the available data for the Pliocene exhibit a cooling trend of 1.5-2.5ºC for this time interval.

Although these corrections may introduce errors in some of our temperature estimates (we expect of the order of 1-2ºC), the overall temperature distribution, represented by the thick line in Fig. 2, is very robust and does not depend on any particular data point. Table S1 combines the original data and the appropriate adjustments.

The SST profile used in GCM simulations for the Pliocene: The SST profile used in boundary conditions for the atmospheric GCM has a generic exponential form with parameters chosen to fit the data in Fig. 2. The equation takes the form:

$$T(\theta) = (T_{\max} - T_{\min}) \exp\left[\frac{1}{a}\left(\frac{|\theta|}{45}\right)^{N}\right] + T_{\min} \qquad (1)$$

where θ is the latitude in degrees, T_{min} is the temperature of freezing for sea water (set to 1.8ºC). T_{max} is the maximum temperature in the tropics (set to 28.5ºC). *N* is set to 4.5; while constant *a* is determined by a least-squares fit to the temperature estimates in Fig. 2. The value of *a* differs in the Atlantic from the rest of globe to allow for warmer temperatures in the North Atlantic:

$$a = \begin{cases} 4.2 \Rightarrow \theta \geq 270, \phi \geq 0 \\ 2.6 \Rightarrow otherwise \end{cases} \qquad (2)$$

To replicate the annual cycle, the SST profile is shifted along the meridian seasonally to match the progression of the modern annual cycle.

To simulate the effect of the Peru Current along the coast of South America, which was warmer than at present but still colder than the surrounding waters (*8*), we add a cold temperature anomaly, T_{Peru}, to our SST profile:

$$T_{Peru} = \begin{cases} -3\cos^2\left[90\,\frac{\phi + 65}{30}\right]\cos^2\left[90\,\frac{\theta + 30}{30}\right] \Rightarrow -75 \leq \theta \leq 15, -110 \leq \phi \leq -65 \\ 0 \Rightarrow otherwise \end{cases} \qquad (3)$$

The SST tropical pattern given by equations (1-3) is shown in Figure S1.

Details of atmospheric GCM simulations: The model simulations were performed using the Community Atmosphere Model (CAM3, *S4*) developed by the National Center for Atmospheric Research (NCAR). It is a three-dimensional spectral model of global extent, with 26 vertical levels and a horizontal truncation of T42 (~2.8º transform grid). We use the model set-up as described by Hack et al. (*S5*). The model source code and the present-day climatogical boundary conditions are freely accessible on the Earth System Grid (www.earthsystemgrid.org).

The model has been spun up for 15 months, after which it has reached dynamic equilibrium. The simulations are then integrated for another decade – the results presented are the average of these final 10 years. The simulation of the modern climate has an atmospheric heat transport across the

equator (Fig. S2). Although this is a feature of the real climate system, it is exaggerated by the model's coarse meridional resolution near the equator.

For the early Pliocene run, we use the reconstructed SST profile as the surface boundary condition and also introduce several other modifications based on the PRISM reconstruction (*21*); including the removal of the Greenland ice sheet, a reduction in the height of the Rockies, Andes and Indonesia to their suggested early Pliocene altitudes, and changes in the Arctic vegetation. A fractional sea ice cover was introduced between the seawater freezing point (T_{min}) and 0ºC. Sensitivity studies have shown that the impact of the imposed SST profile on the Hadley circulation is an order of magnitude larger than the impact of other model modifications (Table S2).

The radiative fluxes quoted in the main body of the paper are derived from the top-of-atmosphere (TOA) fluxes diagnosed by the model and the surface temperatures. The TOA fluxes are divided into clear-sky net longwave, clear-sky net shortwave and cloudy net flux. The radiative response to the increased surface temperatures is calculated assuming blackbody radiation. The water vapour response is computed as the residual of the clear-sky longwave minus the increase blackbody radiation. Inclusion of a more realistic longwave emissivity does not significantly alter the proportions of warming explained by water vapor and cloud feedbacks.

Atmospheric CO_2 concentrations measured in 1990 (355ppm) are used for both Pliocene and present-day simulations (*3*). The atmospheric and oceanic contributions to the heat transport implied by the model are calculated by evaluating heat fluxes at the top of the atmosphere and at the ocean surface (Fig. S3).

Details of coupled GCM simulations: The coupled simulations were performed using the third version of NCAR's Community Climate System Model (CCSM3). This GCM incorporates the atmospheric component described above (CAM3) coupled to ocean and sea ice models (POP and CSIM, respectively). CCSM3 has been used extensively for climate simulations which contributed, for example, to the IPCC Fourth Assessment Report (*S6*). A comprehensive description of the model can be found in Collins *et al.* (*S7*). The model source code and the boundary conditions are freely accessible on the Earth System Grid (www.earthsystemgrid.org).

The experiments discussed in this paper start from an equilibrated preindustrial climate. Two runs are initialized with an instantaneous increase of atmospheric CO_2 concentrations to 355ppm (the level of 1990). The first run uses the standard model set-up, whilst the other has ocean background vertical diffusivity (increased by a factor of 10 in the top 400m, between 40^oS and 40^oN). Both runs have been spun-up for 120 years, and an average of the last 20 years is chosen to make the comparison in Fig. 5.

Figures (Supplementary Online Material)

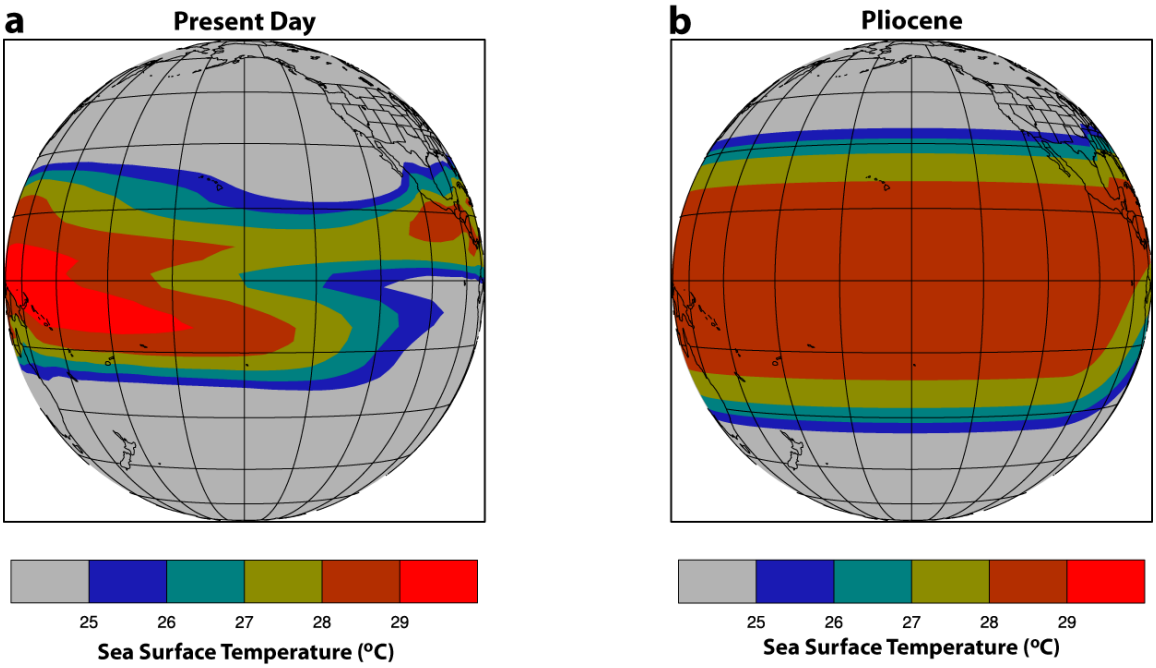

Figure S1. Patterns of mean tropical SSTs showing the extent of the ocean warm pool for the present and early Pliocene climates. The idealized Pliocene SSTs are based on equations (1-3) and the data in Fig. 2.

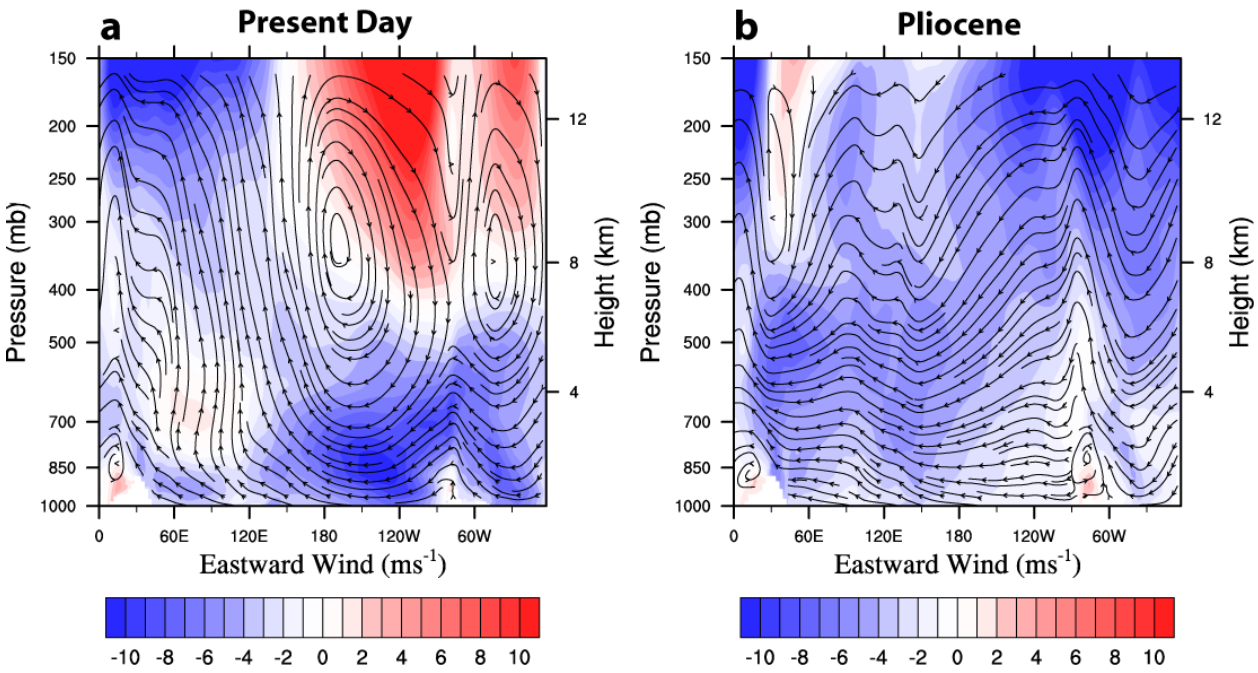

Figure S2. The equatorial circulation in the atmospheric GCM for (a) the present climate and (b) the early Pliocene climate. Instantaneous flow streamlines and the strength of zonal winds (in m/s) in the equatorial plane are shown. Vertical motion has been scaled by a factor of 10^3, so it would appear of the same magnitude as the horizontal motion. The Walker Circulation, evident in the left panel between 150^{o}E and 80^{o}W, is absent in the Pliocene simulation. There is also a corresponding weakening of the low level easterly winds over the equatorial Pacific (from roughly 10 ms^{-1} to 2 ms^{-1}).

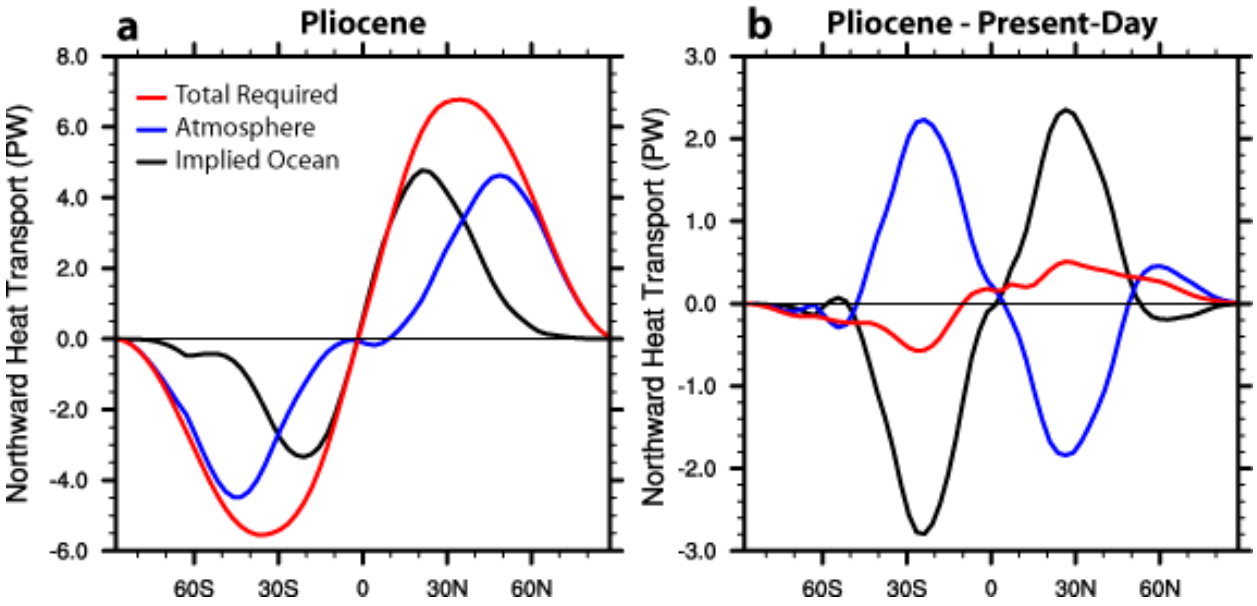

Figure S3. (a) The poleward heat transports simulated in the Pliocene experiment by the atmospheric GCM. Red line: total poleward heat transport. Blue line: atmospheric transport. Black line: implied oceanic heat transport. (b) Differences in these transports between the Pliocene and the present-day climate (shown with the same line colors). For the early Pliocene, the calculations show a slight increase in total poleward heat transport and a strong increase in implied oceanic heat transport.

Reference	Method	Site	Location	Lat.	Lon.	Averaging Interval	Local SST for interval (°C)	Temporal correction (°C)	Location correction (°C)	Est. SST (°C) for the mid-
Atlantic:										
Herbert and Schuffert 1998	Alken.	ODP 958A	NW African margin	23°N	20°W	4-4.3Ma	26.5		+1	27.5
This study	Alken.	DSDP 607	N Atlantic	41°N	33°W	3.9-4.1Ma	21.5		-4	17.5
Bartoli et al. 2005	Mg/Ca	DSDP 609	N Atlantic	50°N	24°W	2.8-3.3Ma	15	+2	-4	13
This study	Alken.	ODP 982	N Atlantic	58°N	16°W	3.9-4.1Ma	17.5		-4	13.5
Bartoli et al. 2005	Mg/Ca	ODP 984	N Atlantic	61°N	24°W	2.8-3.1Ma	10	+2	-4	8
Marlow et al. 2000	Alken.	ODP 1084	SW African margin	26°S	13°E	4-4.3Ma	26.5		+1	27.5
This study	Alken.	ODP 1090	S Atlantic	42°S	8°E	2.5-3.1Ma	13.5	+2	+4	19.5
Pacific:										
Fedorov et al. 2006	Alken	ODP 847	E Eq Pacific	0°	95°W	4-4.3Ma	28			28
Wara et al. 2005	Mg/Ca	ODP 847	E Eq Pacific	0°	95°W	4-4.3Ma	28			28
Wara et al. 2005	Mg/Ca	ODP 806	W Eq Pacific	0°	159°E	4-4.3Ma	28			28
Lawrence et al. 2006	Alken.	ODP 846	E Eq Pacific	3°S	91°W	4-4.3Ma	27		+1	28
Groeneveld et al. 2006, calibrated by Dekens et al. 2007	Mg/Ca	ODP 1241	E Eq Pacific	3°N	88°W	4-4.3Ma	28.5			28.5
Tian et al. 2006	Mg/Ca	ODP 1143	S China Sea	9°N	113°E	3.1-3.3Ma	28.5			28.5
This study	Alken.	ODP 1012	Calif margin	32°N	118°W	3.9-4.1Ma	24.5		+1	25.5
Fedorov et al. 2006, Dekens et al. 2007	Alken.	ODP 1014	Calif margin	33°N	120°W	4-4.3Ma	25		+1	26
Haug et al. 2005	Alken.	ODP 882	N Pacific	50°N	167°E	2.8-3.2Ma	10.5	+2	+1	13.5
Indian:										
Dekens 2007 (PhD thesis)	Mg/Ca	ODP 758	Indian	5°N	90°E	3-5Ma	27.5			27.5

Table S1: SST estimates used in reconstructing the meridional temperature distribution in the Pacific during the early Pliocene (Fig. 2), including references, methods, site locations, and temperature corrections when appropriate.

	Strength of Northern Hadley Cell (10^{10} kg/s)	Strength of Southern Hadley Cell (10^{10} kg/s)
Present-day run (Control)	7.0	9.6
Early Pliocene:		
Standard run (10-year duration)	5.0	4.4
A longer spin-up time (20-year duration)	4.9	4.4
Pliocene SSTs, other surface boundary conditions (e.g. orography, land surface, and ice sheets) as Present-day	5.0	4.5
0.5^{o}C zonal SST gradient imposed along the equator	4.9	4.7
Maximum SST increased to 29^{o}C	5.0	4.5
Pliocene SST profile with slightly altered coefficients in eq. (1) giving faster decrease in SST with latitude (a=2.5, N=4)	5.3	4.8
Tropical Pliocene SSTs merged (between 40^{o} and 60^{o} latitude) with present-day SSTs in high latitudes	5.4	4.6

Table S2: The sensitivity of the strength of the Hadley circulation to changes in the surface boundary conditions. The results show that the reduction in the Hadley Cell intensity is a robust feature of the Pliocene simulations (caused by the strong reduction in the meridional SST gradient).

Location	Present Obs.	Pliocene Paleodata	Present CAM3	Pliocene CAM3	PRISM CAM3	PRISM HadAM3
West Coast USA	459±67	693±300	617±306	536±190	625±249	967±364
East Cost USA	1030	1280	1050	864	1311	676
N. Mediterranean	772±300	1163±110	580±165	647±120	1227±754	830±422
S. Mediterranean	369±28	468±90	91±82	244±136	428±391	418±122
East Africa	692	1000	765	1375	1479	700
China, Shanxi	482	800	1034	1125	1073	1533
China, Yunnan	1389±637	1083±13	1054	1149	1182	1563
NE Australia	1177	2075±601	1097	1643	1178	1075
SE Australia	618±254	2100±458	493±234	768±168	497±159	861±393

Table S3: Comparison of the modelled mean annual precipitation (mm/yr) in several regions to terrestrial paleo-reconstructions. The paleodata, present-day observations and PRISM HadAM3 columns are taken from Table 2 of Salzmann et al. (*25*). The paleodata comes from a variety sources based on palynological inferences (for discussion and references see *25*). The four rightmost columns present the mean annual precipitation as diagnosed using different atmospheric models. "Pliocene CAM3" and "Present CAM3" are the early Pliocene reconstruction and modern control run presented in this work and use version 3 of the Community Atmosphere Model (*S4*). "PRISM CAM3" uses the Pliocene Research, Interpretation and Synoptic Mapping (PRISM) paleoenvironmental reconstruction for the mid-Pliocene (*S8*) as the boundary conditions for a simulation with CAM3. PRISM HadAM3 refers to an atmospheric GCM run (performed by Haywood and Valdes, *S9*) using the 3rd version of the Hadley Centre's Atmosphere Model and incorporating the Mid-Pliocene boundary conditions of Dowsett et al. (*S8*). Differences between the final two columns can be interpreted, in part, as the uncertainty caused by differences in the atmospheric models. The error bars quoted indicate the standard deviation between the individual locations incorporated in the regional average. Note the large uncertainties both in paleo-observations and model simulation. Our Pliocene simulation is also consistent with other qualitative precipitation paleo-observations (*S10*, *S11*)

Supporting Online Material References:

S1. F. G. Prahl, L. A. Muehlhausen, D. L. Zahnle, *Geochim. Cosmochim. Acta* **52**, 2303 (1988).

S2. Shipboard Scientific Party, Site 1012, *Proc. ODP, Init. Repts.* **167**, 129 (1997).

S3. Z. Liu, M. A. Altabet, T. D. Herbert, *Geophys. Res. Lett.* **32**, L23607 (2005).

S4. W. D. Collins *et al., J. Clim.* **19**, 2144 (2006).

S5. J. J. Hack *et al., J. Clim.***19**, 2267 (2006).

S6. D. Randall et al., in *Climate Change 2007: The Physical Science Basis*, S. Solomon et al. (Cambridge University Press, 2007)

S7. W. D. Collins *et al., J. Clim.* **19**, 2122 (2006).

S8. H. J. Dowsett, M. A. Chandler, T. M. Cronin, G. S. Dwyer, *Paleoceanography* **20**, PA2014 (2005). An updated version of this dataset is now available (*21*), however we used the old version to allow comparison to previously published results (*25*).

S9. A. M. Haywood, P. J. Valdes, *Palaeogeogr. Palaeocl.* **237**, 412 (2006)

S10. P. deMenocal, *Earth. Planet. Sc. Lett.* **220**, 3 (2004)

S11. L. M. Dupont, B. Donner, L. Vidal, E. M. Pérez, G. Wefer, *Geology* **33,** 461 (2005)